Two Dimensional Time-Frequency Analysis based Eigenvalue Decomposition Applied to Image Watermarking

Srdjan Stanković, Irena Orović, Nikola Žarić, and Cornel Ioana

Abstract— **An application of two-dimensional time-frequency analysis and corresponding two-dimensional eigenvalue decomposition for image watermarking purpose is proposed. The eigenvalue decomposition is used to provide a criterion for watermarking coefficients selection. It is primarily used to select pixels suitable for watermarking that belong to busy image regions. The watermark embedding is performed in the space/spatial-frequency domain by using middle frequency components, whose number is determined from the eigenvalue decomposition, as well. In order to provide its imperceptibility, watermark is modelled and adapted to the local frequency content of each considered pixel. For an efficient watermark modelling procedure, the concept of space-varying filtering is employed. Furthermore, the watermark detection is done within the space/spatial-frequency domain, which facilitates detection process due to the larger number of coefficients comparing to the space or frequency domain, separately. The efficiency of the proposed procedure and its robustness in the presence of various attacks is proven on the examples.**

I. INTRODUCTION

Digital image watermarking has been developed as a promising approach for intellectual properties protection. The existing image watermarking techniques are mainly based either on spatial or frequency domain [1]-[5]. In the spatial domain, it is very difficult to provide good imperceptibility and robustness. On the other hand, transform domain watermarking techniques (DFT, DCT or DWT) are more efficient in comparison to the spatial domain techniques [3]-[5]. Neverthe-

less, the watermark spreads over all the pixels from a considered region. Additional masking procedure is necessary, in order to make the watermark imperceptible. Consequently, instead of using either spatial or spectral domains for image watermarking, one should use the advantage of both domains by using the joint space/spatial-frequency domain [6]-[9]. The space/spatial-frequency representation is a four-dimensional function and it provides local frequency content estimation for each individual image pixel. Space/spatial-frequency representation provides more space and flexibility for watermark embedding and detection because of its dimensionality [8], [9]. Moreover, since the space/spatial-frequency representations contain information about region dynamics, they can be used to select pixels belonging to busy image regions. These pixels allow embedding of watermark with higher energy without visible quality degradation. Consequently, the appropriate selection of image pixels, improves the imperceptibility and the robustness, as well. Thus, whether a certain pixel will be chosen for watermarking, depends on the number and the energy of its local frequency components within the space/spatial-frequency region [8], [9]. The main problem is to choose a criterion in the space/spatial-frequency domain which will provide efficient pixels selection. In particular, large energy variations of frequency coefficients in a 2D region increase the computational complexity, especially due to empirical thresholds that are difficult to set [9]. Therefore, in this paper, we propose a two-

dimensional eigenvalue decomposition method based on the space/spatial-frequency representation to overcome the aforementioned problem. As a suitable space/spatial-frequency representation, the two-dimensional S-method has been used. First, the eigenvalues are used to determine whether pixels belong to busy or flat image regions. After selecting pixels belonging to busy regions, the eigenvalues are used to determine the support region within space/spatial-frequency representation. This region is then used for watermark modelling, embedding and detection. The inversion from the space/spatial-frequency domain is done by using the concept of space-varying filtering. Using the proposed approach, a two-dimensional space/spatial-frequency region is assigned to each selected pixel, leading to a significantly improved detector performance. Finally, the proposed procedure is tested on various images, providing successful results under different attacks.

The paper is organized as follows. The theoretical background covering the space/spatial-frequency analysis and space-varying filtering is given in Section 2. The eigenvalue decomposition based on the space/spatial-frequency distribution is presented in Section 3. In Section 4, the proposed approach is applied to image watermarking. The efficiency of the proposed watermarking procedure is analyzed experimentally in Section 5. The concluding remarks are given in Section 6.

II. Theoretical Background – Two-Dimensional Time-Frequency Analysis

This section covers the basic theory behind the space/spatial-frequency analysis and the space varying filtering that are crucial for understanding of the proposed approach.

A. Space/Spatial-Frequency analysis

The simplest time-frequency representation is obtained by using the spectrogram, which is defined as a square module of the short-time Fourier transform (STFT). For the sake of simplicity, the vector notation is used. Thus, the spectrogram for two-dimensional signal $s(x, y) = s(\overrightarrow{r})$, can be written as [10]:

$$SPEC(\overrightarrow{r}, \overrightarrow{\omega}) = |STFT(\overrightarrow{r}, \overrightarrow{\omega})| =$$

$$= \left| \int\limits_{R^2} s(\overrightarrow{r} + \overrightarrow{v}) w^*(\overrightarrow{v}) e^{-j\overrightarrow{\omega}\,\overrightarrow{v}} dV_{\overrightarrow{v}} \right|, \quad (1)$$

where $w^*(\overrightarrow{v})$ is a complex conjugate of two-dimensional window function, while $dV_{\overrightarrow{v}}$ is the two-dimensional differential of space R^2. Due to the presence of second and higher order phase derivatives, the spectrogram cannot provide a satisfying concentration at the local frequency. Thus, to improve concentration in the time-frequency domain, the Wigner distribution has been used [10]:

$$WD(\overrightarrow{r}, \overrightarrow{\omega}) =$$

$$= \int\limits_{R^2} s(\overrightarrow{r} + \overrightarrow{v}/2) s^*(\overrightarrow{r} + \overrightarrow{v}/2) e^{-j\overrightarrow{\omega}\,\overrightarrow{v}} dV_{\overrightarrow{v}}.$$

$$(2)$$

However, for multicomponent signals the Wigner distribution contains a large amount of cross-terms. The S-method has been introduced with a goal to preserve the concentration as in the Wigner distribution, but to provide a control of cross-terms number [10]. The S-method can be defined as [10], [11]:

$$SM(\overrightarrow{r}, \overrightarrow{\omega}) =$$

$$= \frac{1}{\pi^2} \int\limits_{R^2} P(\overrightarrow{\theta}) \{ STFT(\overrightarrow{r}, \overrightarrow{\omega} + \overrightarrow{\theta}) \times$$

$$\times STFT(\overrightarrow{r}, \overrightarrow{\omega} - \overrightarrow{\theta}) \} dV_{\overrightarrow{\theta}}. \quad (3)$$

It improves the concentration of spectrogram towards the concentration of the Wigner distribution [12]. For $P(\overrightarrow{\theta}) = 2\pi\delta(\overrightarrow{\theta})$ the spectrogram is obtained, while for $P(\overrightarrow{\theta}) = 1$, the pseudo Wigner distribution follows. The discrete form of the S-method can be written as:

$$SM(\overrightarrow{n}, \overrightarrow{\omega}) =$$

$$= \sum_{i_1=-L}^{L} \sum_{i_2=-L}^{L} P(\overrightarrow{i}) \{ STFT(\overrightarrow{n}, \overrightarrow{\omega} + \overrightarrow{i}) \times$$

$$\times STFT^*(\overrightarrow{n}, \overrightarrow{\omega} - \overrightarrow{i}) \}$$

$$= SPEC(\overrightarrow{n}, \overrightarrow{\omega}) +$$

$$+2Re\Big\{ \sum_{i_1=0}^{L} \sum_{i_2=0}^{L} P(\overrightarrow{i}) \big\{ STFT(\overrightarrow{n}, \overrightarrow{\omega} + \overrightarrow{i}) \times$$

$$\times STFT^*(\overrightarrow{n}, \overrightarrow{\omega} - \overrightarrow{i}) \big\} \Big\}, \qquad (4)$$

where $\overrightarrow{n} = (n_1, n_2), \overrightarrow{\omega} = (\omega_1, \omega_2)$ and $\overrightarrow{i} = (i_1, i_2)$. The frequency window $P(i_1, i_2)$ is a rectangular separable window of width $2L+1$ in both directions, while the discrete STFT is given by:

$$STFT(\overrightarrow{n}, \overrightarrow{\omega}) =$$

$$= \sum_{k_1=-\frac{N}{2}}^{\frac{N}{2}-1} \sum_{k_2=-\frac{N}{2}}^{\frac{N}{2}-1} I(\overrightarrow{n} + \overrightarrow{k}) w^*(\overrightarrow{k}) e^{-j2\pi \overrightarrow{\omega} \overrightarrow{k}/N},$$

$$(5)$$

for $\overrightarrow{k} = (k_1, k_2)$. In most applications, it is sufficient to use small value of L in (4) (e.g., L=3) [12].

B. Space-varying filtering

Although, it was initially introduced for signals denoising, the concept of non-stationary filtering can be used to provide inversion from the time-frequency or space/spatial-frequency domain. The output of the space-varying filter is defined as:

$$H_s(\overrightarrow{r}) = \frac{1}{4\pi^2} \int\limits_{\overrightarrow{\omega}} L_H(\overrightarrow{r}, \overrightarrow{\omega}) STFT_s(\overrightarrow{r}, \overrightarrow{\omega}) d\overrightarrow{\omega},$$

$$(6)$$

where $L_H(\overrightarrow{r}, \overrightarrow{\omega})$ is a space-varying transfer function (i.e., support function) defined as Weyl symbol mapping of the impulse response into the space/spatial-frequency domain [11]. Assuming that the signal components are contained within a two-dimensional region R_f, the support function $L_H(\overrightarrow{r}, \overrightarrow{\omega})$ can be defined as [11]:

$$L_H(\overrightarrow{r}, \overrightarrow{\omega}) = \begin{cases} 1 & \text{for} \quad (\overrightarrow{r}, \overrightarrow{\omega}) \in R_f \\ 0 & \text{for} \quad (\overrightarrow{r}, \overrightarrow{\omega}) \notin R_f \end{cases}. \quad (7)$$

The proposed watermarking procedure implements the space-varying filtering (masking) to retrieve watermarked signal from the space/spatial-frequency domain.

III. EIGENVALUE DECOMPOSITION BASED ON THE SPACE/SPATIAL-FREQUENCY DISTRIBUTION

The S-method produces a representation equal (or close) to a sum of the Wigner distributions of signal components separately. This property is used to introduce an eigenvalue decomposition method [13], extended here for the case of two-dimensional signals. Thus, let us start from the discrete form of the two-dimensional Wigner distribution:

$$WD(\overrightarrow{n}, \overrightarrow{k}) =$$

$$= \sum_{\overrightarrow{m}=-N/2}^{N/2} s(\overrightarrow{n} + \overrightarrow{m}) s^*(\overrightarrow{n} - \overrightarrow{m}) e^{-j\frac{2\pi}{N+1} 2\overrightarrow{m}\overrightarrow{k}},$$

$$(8)$$

where $\overrightarrow{n} = (n_1, n_2)$ and $\overrightarrow{k} = (k_1, k_2)$ represents discrete time and frequency samples, while $\overrightarrow{m} = (m_1, m_2)$ is a discrete lag coordinate. Consequently, the inverse of the Wigner distribution can be written as:

$$s(\overrightarrow{n_1}) s^*(\overrightarrow{n_2}) = \frac{1}{(N+1)^2} \times$$

$$\times \sum_{\overrightarrow{k}=-N/2}^{N/2} WD(\frac{\overrightarrow{n_1} + \overrightarrow{n_2}}{2}, k) e^{j\frac{2\pi}{N+1} \overrightarrow{k}(\overrightarrow{n_1} - \overrightarrow{n_2})}$$

$$(9)$$

where $\overrightarrow{n}_1 = \overrightarrow{n} + \overrightarrow{m}$ and $\overrightarrow{n}_2 = \overrightarrow{n} - \overrightarrow{m}$. Furthermore, for a multicomponent signal, $s(\overrightarrow{n}) = \sum_{i=1}^{M} s_i(\overrightarrow{n})$, (9) can be written as:

$$\sum_{i=1}^{M} s_i(\overrightarrow{n_1}) s_i^*(\overrightarrow{n_2}) = \frac{1}{(N+1)^2} \times$$

$$\times \sum_{\overrightarrow{k}=-\frac{N}{2}}^{\frac{N}{2}} \sum_{i=1}^{M} WD_i(\frac{\overrightarrow{n_1} + \overrightarrow{n_2}}{2}, \overrightarrow{k}) e^{j\frac{2\pi}{N+1} \overrightarrow{k}(\overrightarrow{n_1} - \overrightarrow{n_2})}.$$

$$(10)$$

Given that the S-method of $s(\overrightarrow{n})$ is equal to the sum of the Wigner distributions of each component separately, $SM(\overrightarrow{n}, \overrightarrow{k}) = \sum_{i=1}^{M} WD_i(\overrightarrow{n}, \overrightarrow{k})$, (10) can be rewritten as:

$$\sum_{i=1}^{M} s_i(\overrightarrow{n_1}) s_i^*(\overrightarrow{n_2}) = \frac{1}{(N+1)^2} \times$$

$$\times \sum_{\overrightarrow{k}=-N/2}^{N/2} SM(\frac{\overrightarrow{n_1}+\overrightarrow{n_2}}{2}, \overrightarrow{k})e^{j\frac{2\pi}{N+1}\overrightarrow{k}(\overrightarrow{n_1}-\overrightarrow{n_2})}.$$

(11)

By introducing the notation:

$$R_{SM}(\overrightarrow{n_1}, \overrightarrow{n_2}) = \frac{1}{(N+1)^2} \times$$

$$\times \sum_{\overrightarrow{k}=-N/2}^{N/2} SM(\frac{\overrightarrow{n_1}+\overrightarrow{n_2}}{2}, \overrightarrow{k})e^{j\frac{2\pi}{N+1}\overrightarrow{k}(\overrightarrow{n_1}-\overrightarrow{n_2})},$$

(12)

we have: $R_{SM}(\overrightarrow{n_1}, \overrightarrow{n_2}) = \sum_{i=1}^{M} s_i(\overrightarrow{n_1})s_i^*(\overrightarrow{n_2})$. The eigenvalue decomposition of matrix R_{SM} is defined as [13]:

$$R_{SM} = \sum_{i=1}^{N+1} \lambda_i u_i(\overrightarrow{n})u_i^*(\overrightarrow{n}),$$

(13)

where λ_i are eigenvalues and $u_i(\overrightarrow{n})$ are eigenvectors of R_{SM}. Furthermore, $\lambda_i = E_{f_i}$, $i = 1,,...,M$ and $\lambda_i = 0$ for $i = M+1,...,N$, i.e,

$$\lambda_i = \sum_{l=1}^{M} E_{f_i}\delta(i-l),$$

(14)

where $\delta(i)$ denotes Kronecker symbol, while E_{f_i} is the energy of the i-th component.

IV. WATERMARKING PROCEDURE

A. Classification of image regions

Pixels within busy image regions (regions with significant dynamics), could tolerate greater changes (stronger watermark) without a perceptible quality degradation than the pixels from the flat regions. Thus, in order to provide good imperceptibility and robustness, simultaneously, the appropriate selection of pixels is an important issue. For this purpose, we can use a space/spatial-frequency representation that is able to emphasize the regions' dynamics. Due to its good properties, a space/spatial-frequency representation is obtained by using the two-dimensional S-method. It improves the concentration comparing to the spectrogram. Also, complexity of the realization does not significantly increase, since the S-method is based on the short-time Fourier transform, as well. Note that the number of components in the S-method is related
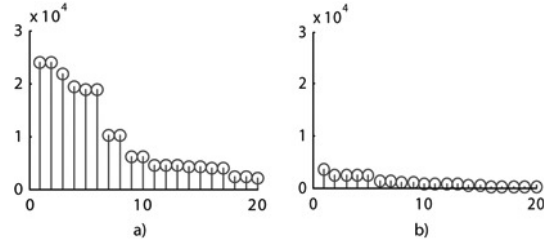
Fig. 1. Eigenvalues corresponding to: a) busy region, b) flat region

to the number of eigenvalues and eigenvectors. Thus, the eigenvalues will be used for pixels classification.

In order to classify whether pixels belong to flat or busy regions, we can implement the following steps:

Step 1) The two-dimensional short-time Fourier transform is calculated according to (5) by using $N=20$. Thus, the region of size 20x20 is considered around each pixel.

Step 2) Based on the short-time Fourier transform, the S-method is calculated for the central pixel $(n_1, n_2)$of the considered region according to (4), and it is denoted as $SM_{n_1,n_2}(\omega_1, \omega_2)$. The low frequency content is removed from $SM_{n_1,n_2}(\omega_1, \omega_2)$, to avoid the influence of luminance component, and to highlight details (dynamics of the region) located at the middle frequencies.

Step 3) The R_{SM} matrix is calculated for each $SM_{n_1,n_2}(\omega_1, \omega_2)$

Step 4) Decompose R_{SM} into eigenvalues and eigenvectors.

Step 5) The eigenvalues $\lambda_{n_1,n_2}(i)$, i=1,... M, obtained for the central pixel (n_1, n_2) are then used for classification. In other words, the eigenvalues corresponding to the flat region should be significantly smaller than those from the busy regions (Fig 1).

By assuming a floor value λ_0, a support vector can be defined as:

$$\xi(i) = \begin{cases} 1, & \lambda_{n_1,n_2}(i) > \lambda_0 \\ 0, & otherwise. \end{cases}$$

(15)

Then, the testing hypothesis could be defined as:

$$\Xi = \sum_{i=1}^{M} \xi(i) \begin{array}{c} \overset{h1}{>} \xi_0 \\ \underset{h2}{\leq} \xi_0 \end{array} , \qquad (16)$$

where $h1$ assumes a busy region, while $h2$ assumes a flat region. Furthermore, the value λ_0 should provide a clear difference between Ξ for busy and Ξ for flat regions, so that the threshold ξ_0 can be easily set. Thus, numerous experiments have been performed (with different images and regions) in order to determine the optimal value of λ_0. It has been shown that for $\lambda_0 = 0.5 \cdot 10^4$, Ξ is either 0 or 1 for all tested flat regions. On the other hand, for busy regions, Ξ achieves significantly larger values. Some illustrative examples are reported in Table 1. Note that there is a significant gap between values of Ξ for busy and flat regions providing precise pixels classification. Thus, ξ_0 could be set between the lowest Ξ obtained for busy regions and the highest Ξ for flat regions. It is important to note that the classification can be performed by using small number of eigenvectors, e.g. $M{=}20$, which is more efficient and faster than the method presented in [9].

Choosing a proper value of N is also essential for the proposed algorithm. In particular, $N{=}20$ was found to be optimal region size for these applications. Otherwise, regions either contain a mixture of busy and flat regions, or do not contain sufficient information.

B. Watermark modelling procedure

In order to provide its imperceptibility, the space/spatial-frequency characteristics of the watermark should be adjusted to the space/spatial-frequency coefficients of the host signal [8]. Modelling of the watermark is based on the trade-off between the robustness and the imperceptibility. A watermark modelled according to the low-frequency-high-energy components is robust, but may cause perceptual degradation. On the other side, a watermark modelled according to the high frequency components will not be robust enough.

Thus, in order to fulfil both the imperceptibility and robustness, the middle frequency region is considered for watermarking:
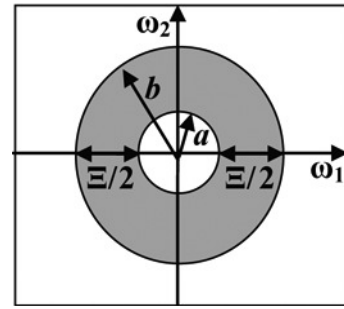
Fig. 2.   Illustration of the middle frequency region within (ω_1, ω_2)

$$D = \left\{ (\omega_1, \omega_2) : a^2 < \omega_1^2 + \omega_2^2 < b^2 \right\}, \quad (17)$$

where, $b - a = \left\lceil \frac{\Xi}{2} \right\rceil$.

The region D will be called the support region and it is illustrated in Fig 2. The parameter a denotes the width of the low frequency region that should be avoided.

Note that the width of region D will change depending on the number of eigenvalues Ξ, selected by (15). A greater value Ξ reflects higher number of significant components and vice versa. Further, it has been experimentally shown that the total width of frequency region D could be approximately tied to Ξ (Fig 2). Thus, each frequency region will offer certain number of components depending on its dynamics i.e. depending on Ξ.

Further, the short-time Fourier transform of a starting 2-D pseudo-random sequence is used to obtain the watermark whose space/spatial frequency characteristics will be modelled according to the region D:
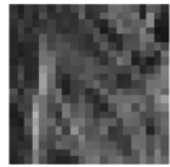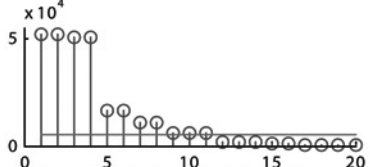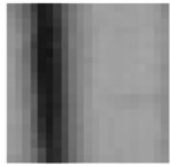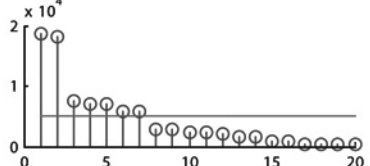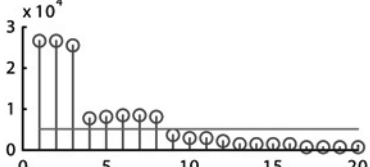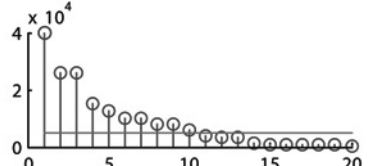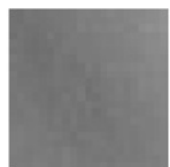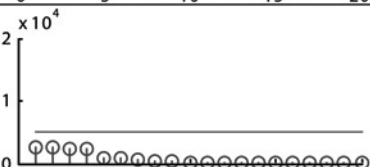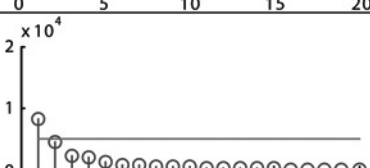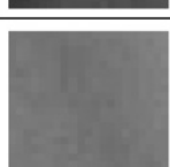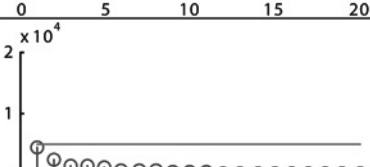
$$STFT_{wat}(n_1, n_2, \omega_1, \omega_2) = \beta \cdot STFT_p(D), \tag{18}$$

where $STFT_p$ is the short-time Fourier transform of a pseudo-random sequence, while $STFT_{wat}$ is the resulting short-time Fourier transform of the watermark. The parameter β controls the watermark strength.

C. Watermark embedding and detection procedure

A watermark embedding procedure is performed in the space/spatial frequency domain,

TABLE I
The results of eigenvalue decomposition for different image regions

Image region		S-method	Eigenvalues	
Busy				$\Xi=11$
Busy				$\Xi=7$
Busy				$\Xi=8$
Busy				$\Xi=10$
Flat				$\Xi=1$
Flat				$\Xi=0$
Flat				$\Xi=1$
Flat				$\Xi=0$

as follows [8], [9]:

$$STFT_{Iw}(n_1, n_2, \omega_1, \omega_2) =$$
$$= STFT_I(n_1, n_2, \omega_1, \omega_2) +$$
$$+ STFTwat(n_1, n_2, \omega_1, \omega_2), \qquad (19)$$

where $STFT_I$ and $STFT_{Iw}$ are the short-time Fourier transforms of the original and watermarked image, respectively.

In order to retrieve the signal from its space/spatial-frequency representation, the concept of space-varying filtering/masking is applied. Input of the space-varying filter is $STFT_{Iw}$, while the support function is defined as:

$$L(\omega_1, \omega_2) = \begin{cases} 1 & \text{if} \quad |SM_I(\omega_1, \omega_2)| > 0 \\ 0 & \text{otherwise.} \end{cases}$$
$$(20)$$

The watermarked image pixel on the position (n_1, n_2) is obtained as [8]:

$$Iw(n_1, n_2) =$$
$$= \frac{1}{2\pi} \sum_{\omega_1} \sum_{\omega_2} STFT_{Iw}(n_1, n_2, \omega_1, \omega_2) L(\omega_1, \omega_2).$$
$$(21)$$

Following the similar concept as in the embedding process, the watermark detection is performed, within a region D, by using the standard correlation detector in the space/spatial-frequency domain:

$$Det = \sum_{i=1}^{N_w} \left[\sum_{\omega_1} \sum_{\omega_2} STFT_{I_w}(D) STFT_{w_{key}}(D) \right],$$
$$(22)$$

where N_w is the total number of pixels selected for watermarking. Since, the two-dimensional space/spatial-frequency region is assigned to each selected pixel, the actual number of components used in the detection procedure is for one order larger, providing a significant detection improvement. The detection performance is tested by using the following measure of detection quality [14], [15]:

$$R = \frac{\overline{D}_{w_r} - \overline{D}_{w_w}}{\sqrt{\sigma_{w_r}^2 + \sigma_{w_w}^2}}, \qquad (23)$$
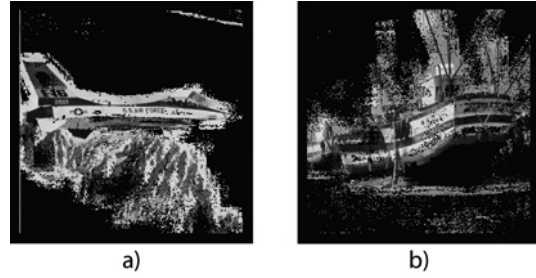

Fig. 3. The pixels from busy image regions selected according to the proposed procedure: a) F16, b) Boat

where $\overline{D}$ and σ^2 represent the mean value and the standard deviation of the detector responses, while notations w_r and w_w indicate the right and wrong keys (trials), respectively. The probability of error P_{err} can be easily calculated by using measure R, as follows:

$$P_{err} = \frac{1}{2} erfc(\frac{R}{\sqrt{2}}). \qquad (24)$$

The normal distribution of detector's responses is assumed. Probability of detection is obtained as $P_d = 1 - P_{err}$. By increasing the value of measure R the probability of detection error decreases.

V. Experimental Results

The advantages of the proposed watermarking procedure are shown in this Section. The various images are used in the experiments. The STFT is calculated by using the regions 20x20 pixels, while the S-method is done with $L=3$. The pixels belonging to the busy image regions are determined according to the proposed procedure. The selected pixels of images F16 and Boat are given in Fig 3 (black points are omitted). The watermark is modeled according to (18) providing high PSNR=50dB. The procedure is tested for various images and we report the results for some of them. The results are very similar for other images, as well. The procedure is compared with procedures performed in spatial domain (Spatial procedure), frequency domain (DCT procedure), and space/spatial-frequency based procedure in [9].

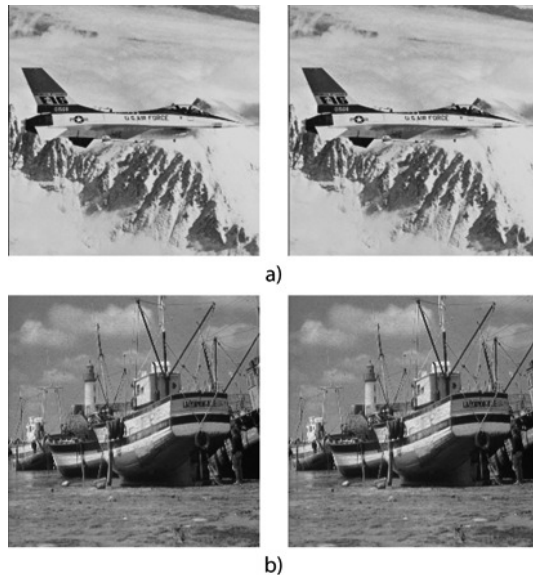Note that the comparison is done under the

Fig. 4. Original (left) and Watermarked (right) image: a) F16, b) Boat

Fig. 5. Comparison of measures of detection quality R for different procedures and different images

same PSNR using the same number of watermarked pixels: for image Lena – 4330 pixels, Peppers – 4830, F16 – 3304, Boat – 6015 pixels, etc.

The original and watermarked images Boat and F16 are shown in Fig 4. Furthermore, the detection is performed within the corresponding domain (spatial, DCT domain or space/spatial-frequency domain) by using the form of correlation detector for each procedure. The results of watermark detection are given in Fig 5.

The measures of detection quality are calculated and they are graphically presented. Note that the proposed procedure provides the highest value of R, leading to the lowest probability of error. For each considered pixel, the proposed procedure has a number of middle frequency components on disposal. This number of components is adjusted to the region dynamics and it depends on how busy the region is. Thus, it can provide successful results and improvements comparing to other domains, even when relatively small number of pixels is considered.

Additionally, the procedure is tested under some commonly applied attacks, such as: JPEG compression with quality 80, JPEG
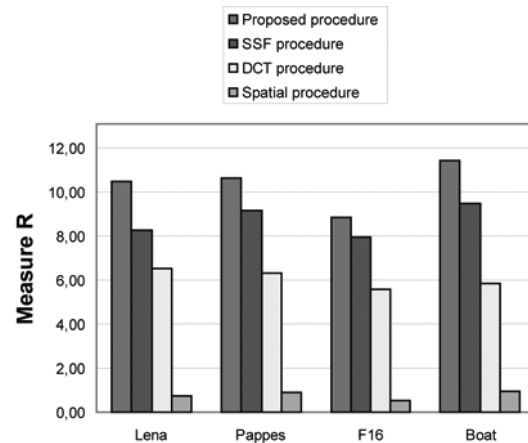
compression with quality 50, impulse noise, Gaussian noise, median filtering with mask 3x3, and average filter 3x3. The results for a few of tested images are given in Fig 6.

One might observe that the proposed procedure provides better results even under attacks. Observe that, the lowest measure of detection quality is obtained for median filtering procedure: the average value of R for different test images is $R \approx 5$, and its average probability of error is $P_e \sim 10^{-7}$.

VI. CONCLUSION

Space/spatial-frequency analysis and the corresponding eigenvalue decomposition method have been applied to provide an efficient image watermarking method. The space/spatial-frequency representation is obtained by using the two-dimensional S-method. It has been shown that the proposed eigenvalue decomposition leads to an efficient procedure that classifies pixels belonging to busy and flat regions. Only the local frequency content corresponding to pixels from busy regions are considered for watermarking, providing better imperceptibility. Furthermore, the middle frequency components are used, while their number is also adapted to the dynamics of the region. The space/spatial-frequency content of the watermark is modelled according to selected spectral components. Finally, the proposed pixel selection method, together with
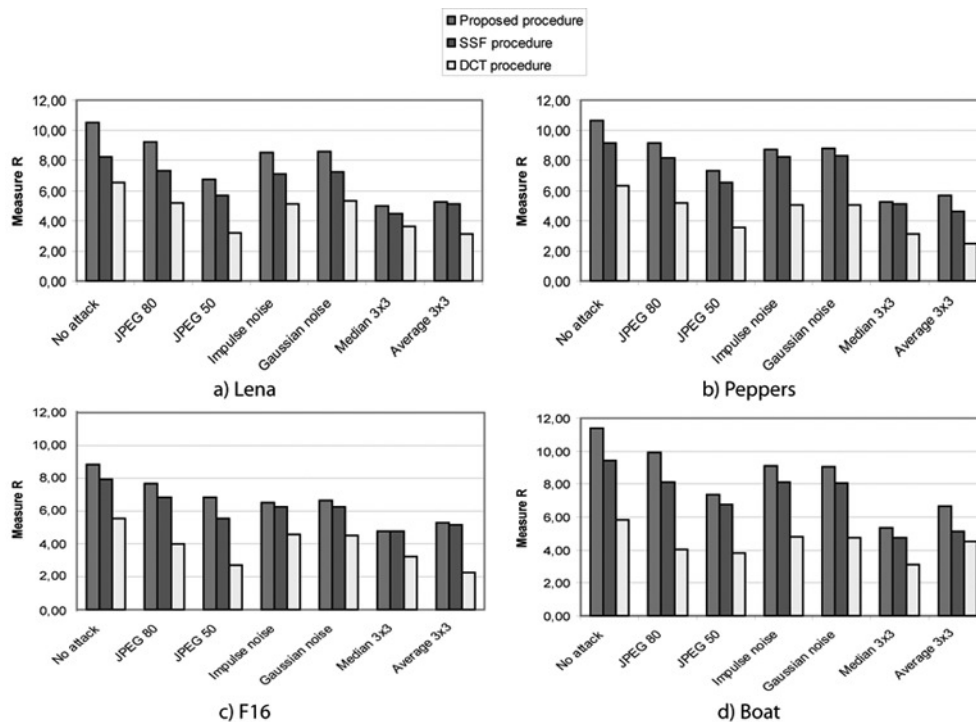
Fig. 6. Measures of detection quality under different attacks: a) Lena, b) Peppers, c) F16, d) Boat

watermark modelling procedure, have been reflected to the successful detection process, based on the large number of coefficients in the space/spatial-frequency domain.

ACKNOWLEDGEMENT

REFERENCES

[1] J. Cox, M. L. Miller, J. A. Bloom, *Digital Watermarking*, Kaufmann, San Francisco, 2002.

[2] M. Barni, F. Bartolini, *Watermarking Systems Engineering*, Marcel Dekker, New York, 2004.

[3] E. Muharemagić, B. Furht, "Survey of Watermarking Techniques and Applications," In: Furht B and Kirovski D (ed) Multimedia Watermarking Techniques and Applications. Auerbach Publication, New York, pp. 91-130, 2006.

[4] A. Nikolaidis, I. Pitas, "Asymptotically optimal detection for additive watermarking in the DCT and DWT domains," *IEEE Transactions on Image Processing*, Vol. 12, No. 5, pp. 563-571, 2003.

[5] J. R. Hernandez, M. Amado, F. Perez Gonzales, "DCT-domain watermarking techniques for still images: Detector performance analysis and a new structure," *IEEE Transactions on Image Processing*, Vol. 9, pp. 55-68, 2000.

[6] B. G. Mobaseri, "Digital watermarking in the joint time-frequency domain," *IEEE International Conference on Image Processing*, Sept. 2002, New York, Vol. 3, pp. 481-484.

[7] M. Al-khassaweneh, S. Aviyente, "A time-frequency inspired robust image watermarking," *in IEEE Conference Record of the Thirty-Eighth Asilomar Conference*, Vol. 1, pp. 392-396, 2004.

[8] N. Žarić, I. Orović, S. Stanković, C. Ioana "Space/Spatial-Frequency Based Image Watermarking," in *Proceedings of 50th International Symposium ELMAR 2008*, Zadar, Croatia, pp. 101-104, 2008.

[9] S. Stanković, I. Orović, N. Žarić, "An Application of Multidimensional Time-Frequency Analysis as a base for the Unified Watermarking Approach," *IEEE Transactions on Image Processing*, Vol. 1, No. 3, pp. 736-745, March 2010.

[10] S. Stanković, LJ. Stanković, Z. Uskoković, "On the local Frequency, Group Shift and Cross Terms in Some Multidimensional Time-Frequency Distributions; A Method for Multidimensional Time-Frequency Analysis," *IEEE Transactions on Signal Processing*, Vol. 43, No. 7, pp. 1719-1724, 1995.

[11] LJ. Stanković, S. Stanković, I. Djurović, "Space/Spatial-Frequency Based Filtering," *IEEE Transactions on Signal Processing*, Vol. 48, No. 8, pp. 2343-2352, 2000.

[12] LJ. Stanković, "A method for Time-Frequency Signal Analysis," *IEEE Transactions on Signal Processing*, Vol. 42, No. 1, pp. 225-229, 1994.

[13] LJ. Stanković, T. Thayaparan, M. Daković, "Signal Decomposition by Using the S-method With Application to the Analysis of HF Radar Signals in Sea-Clutter," *IEEE Transactions on Signal Processing*, Vol. 54, No.11, pp. 4332- 4342, 2006.

[14] D. Heeger, *Signal Detection Theory*, Teaching Handout, Department of Psysichs, Stanford University, Stanford, CA, 1997.

[15] T. D. Wickens, *Elementary Signal Detection Theory*, Oxford University Press, Oxford, 2002.